Front. Med. 2022, 16(3): 467–482
https://doi.org/10.1007/s11684-021-0869-y

RESEARCH ARTICLE

Rapamycin enhances the anti-tumor activity of cabozantinib in cMet inhibitor-resistant hepatocellular carcinoma

Chao Gao[1,*], Shenghao Wang[1,*], Weiqing Shao[1], Yu Zhang[1], Lu Lu[1], Huliang Jia[1], Kejin Zhu[2], Jinhong Chen[1], Qiongzhu Dong[1,3], Ming Lu[1], Wenwei Zhu (✉)[1], Lunxiu Qin (✉)[1,3]

[1]*Department of General Surgery, Huashan Hospital, Cancer Metastasis Institute, Fudan University, Shanghai 200040, China;* [2]*Kanion Research Institute, Lianyungang 222002, China;* [3]*Institutes of Biomedical Sciences, Fudan University, Shanghai 200040, China*

Abstract **Cabozantinib, mainly targeting cMet and vascular endothelial growth factor receptor 2, is the second-line treatment for patients with advanced hepatocellular carcinoma (HCC). However, the lower response rate and resistance limit its enduring clinical benefit. In this study, we found that cMet-low HCC cells showed primary resistance to cMet inhibitors, and the combination of cabozantinib and mammalian target of rapamycin (mTOR) inhibitor, rapamycin, exhibited a synergistic inhibitory effect on the *in vitro* cell proliferation and *in vivo* tumor growth of these cells. Mechanically, the combination of rapamycin with cabozantinib resulted in the remarkable inhibition of AKT, extracellular signal-regulated protein kinases, mTOR, and common downstream signal molecules of receptor tyrosine kinases; decreased cyclin D1 expression; and induced cell cycle arrest. Meanwhile, rapamycin enhanced the inhibitory effects of cabozantinib on the migration and tubule formation of human umbilical vascular endothelial cells and human growth factor-induced invasion of cMet inhibitor-resistant HCC cells under hypoxia condition. These effects were further validated in xenograft models. In conclusion, our findings uncover a potential combination therapy of cabozantinib and rapamycin to combat cabozantinib-resistant HCC.**

Keywords hepatocellular carcinoma; cabozantinib; primary resistance; rapamycin

Introduction

Hepatocellular carcinoma (HCC) is the fourth leading cause of cancer-related death globally [1]. Much progress has been obtained in the systemic treatments of advanced-stage HCC [2]. Anti-angiogenic tyrosine kinase inhibitors (TKIs) are the landmark breakthrough in systemic treatments of HCC. Sorafenib and lenvatinib have been demonstrated to prolong the overall survival of patients with unresectable HCC and proved to be the first-line treatment. Nevertheless, the response rate and survival benefits provided by these TKIs are limited [3]. Thus, more effective therapeutic strategies need to be developed.

Human growth factor (HGF)/cMet is a pivotal and clinically actionable pathway. Constitutive cMet activation drives a complex tumor progression program and is involved in sorafenib resistance in HCC [4]. Cabozantinib is an oral small-molecule TKI that mainly blocks the phosphorylation of cMet and vascular endothelial growth factor receptor 2 (VEGFR2), as well as a number of other receptor tyrosine kinases (RTKs) including RET, KIT, AXL, and FLT3 [5]. It exerts its anti-tumor effect via inhibiting angiogenesis, proliferation, and metastasis of HCC cells under hypoxia condition and has been proved to be the second-line treatment for advanced-stage HCC patients [5–7]. However, the lower response rate and the probabilities of drug resistance limit the enduring clinical benefits of cabozantinib [5–7].

Mammalian target of rapamycin (mTOR) is a common and key signal transducing molecule in downstream signaling pathways of RTKs. Sustained mTOR signal confers drug resistance to various targeted therapies. Rapamycin is an allosteric mTORC1 inhibitor and has been approved by the Food and Drug Administration in the treatment of renal cell carcinoma and neuroendocrine tumors [8,9]. However, the anti-tumor effect of rapamycin on patients with unresectable HCC is compromised [10,11].

Our previous study revealed that cMet-low HCC cells showed less sensitivity to cMet inhibitors than cMet-high

Received December 15, 2020; accepted May 28, 2021
Correspondence: Wenwei Zhu, westoolife@163.com;
Lunxiu Qin, qinlx@fudan.edu.cn

[*]These authors contributed equally to this work.

HCC cells [12]. In this study, we further demonstrated that the combination of rapamycin with cabozantinib had a synergistic suppressive effect on the tumor growth and hypoxia-induced metastasis of cMet inhibitor-resistant HCC cells. Mechanically, the combination treatment induced a more effective inhibition of downstream signal pathways of RTKs in cMet inhibitor-resistant HCC cells. This study provides a potential strategy to overcome the primary resistance of HCC to cabozantinib.

Materials and methods

Human clinical samples

Paraffin-fixed human HCC samples were collected from HCC patients who underwent liver resection at the Department of General Surgery, Huashan Hospital, Fudan University. All clinical samples were collected from patients after obtaining informed consent in accordance with a protocol approved by the Ethics Committee of Huashan Hospital, Fudan University (Shanghai, China).

Cell culture

Human HCC cell lines, MHCC-97H and MHCC-97L, were provided by the Liver Cancer Institute, Zhongshan Hospital, Fudan University. Human HCC cell lines including PLC/PRF/5 (PLC), Hep3B, and HepG2 cells were purchased from the American Type Culture Collection. Human umbilical vascular endothelial cells (HUVECs), Huh7, and mouse hepatocarcinoma cell line Hepa1-6 were obtained from the Cell Bank of Type Culture Collection of Chinese Academy of Sciences. All HCC cell lines were cultured in DMEM (Gibco) with 10% (v/v) FBS (Gibco) at 37 °C in a humidified incubator with 5% CO_2. HUVECs were cultured in ECM (ScienCell) with 10% (v/v) FBS (Gibco).

Cell proliferation assay

Cell proliferation was measured by using the Cell Counting Kit-8 (CCK8) according to the manufacturer's instructions (HY-K0301, MCE). Briefly, HCC cells were plated at a density of 3000 cells per well in 96-well plates and incubated for 12 h. Then, cells were treated with the indicated drug concentration for an additional 72 h. About 10 μL of CCK8 reagent was added and incubated for 1 h at 37 °C. The absorbance at 450 nm was measured with a microplate reader (Infinite M200 Pro NanoQuant, TECAN). The inhibitors used for cell proliferation assay included CC930 (S8490, Selleck), SB202190 (S1077, Selleck), sotrastaurin (S2791, Selleck), MK2206 (S1078, Selleck), SCH772984 (S7101, Selleck), rapamycin (HY-10219, MCE), SC75741 (S7273, Selleck), regorafenib (S1178, Selleck), gefitinib (S1025, Selleck), lapatinib (S2111, Selleck), BGJ398 (S2183, Selleck), dasatinib (S1021, Selleck), olaparib (S1060, Selleck), niraparib (S2741, Selleck), MK-1775 (S1525, Selleck), FK866 (S2799, Selleck), palbociclib (S1116, Selleck), obatoclax (S1057, Selleck), GSK525762A (S7189, Selleck), JQ1 (S7110, Selleck), cabozantinib (S1119, Selleck), and NZ001 (Nanjing Zhongrunyuan Pharmaceutical Company). Among these inhibitors, palbociclib was resolved using water, and all other inhibitors were resolved using DMSO for *in vitro* experiments.

Combination index (CI) assay

After treatment with the indicated inhibitors, the cell viability was measured by cell proliferation assay. The drug combination studies and their synergistic interactions were analyzed by CompuSyn software on the basis of the Chou–Talalay method [13]. $CI > 1$ indicated antagonism, $CI = 1$ indicated additivity, and $CI < 1$ indicated synergism between two drugs.

Western blot

To prepare whole cell lysate, HCC cells were lysed with RIPA Lysis Buffer (P0013C, Beyotime) containing protease inhibitors (HY-K0010, MCE) and phosphatase inhibitors (HY-K0021, MCE), and the protein concentration was determined using bicinchoninic acid assay (23225, Thermo Fisher Scientific). Equal amounts of protein were separated by SDS-PAGE and analyzed with primary and secondary antibodies following the manufacturer's protocols. The signals were obtained by using an enhanced chemiluminescence reagent (WBKLS0500, Millipore Corp). The primary antibodies used for Western blot included cMet (8198, Cell Signaling Technology), pMet (Tyr1234/1235) (3077, Cell Signaling Technology), cyclin D1 (ab134175, Abcam), PARP (9532, Cell Signaling Technology), cleaved-PARP (5625, Cell Signaling Technology), GAPDH (AC002, ABclonal), pAKT (Ser473) (4060, Cell Signaling Technology), AKT (4685, Cell Signaling Technology), pmTOR (Ser2448) (5536, Cell Signaling Technology), pmTOR (Ser2481) (2974, Cell Signaling Technology), mTOR (2983, Cell Signaling Technology), pERK1/2 (Thr202/Tyr204) (4370, Cell Signaling Technology), ERK1/2 (4695, Cell Signaling Technology), p-p65 (Ser536) (3033, Cell Signaling Technology), p65 (8242, Cell Signaling Technology), pP70S6K (Thr421/Ser424) (9204, Cell Signaling Technology), P70S6K (9202, Cell Signaling Technology), pEGFR (Tyr1068) (3777, Cell Signaling Technology), EGFR (4267, Cell Signaling Technology), pFGFR2 (Tyr653/654) (3476, Cell Signaling Technology), FGFR2 (23328, Cell Signaling Technology), pERBB2 (Tyr1221/1222) (2243, Cell Signaling Technology), ERBB2 (2165, Cell Signaling Technology), pPLCr (Ser1248) (8713, Cell

Signaling Technology), PLCr (2822, Cell Signaling Technology), pMEK (Ser221) (2338, Cell Signaling Technology), MEK (4694, Cell Signaling Technology), pJAK2 (Tyr1007/1008) (3771, Cell Signaling Technology), and JAK2 (3230, Cell Signaling Technology). The secondary antibodies used for Western blot included HRP Goat Anti-mouse IgG (AS003, ABclonal) and HRP Goat Anti-rabbit IgG (AS014, ABclonal).

Cell cycle and apoptosis

After treatment with the indicated inhibitors for 48 h, the cells were washed with PBS buffer twice and collected (1×10^5). Cell cycle and apoptosis were analyzed using flow cytometry with propidium iodide/RNase staining buffer (550825, BD Biosciences, USA) and annexin V-FITC/PI apoptosis detection kits (556547, BD Biosciences, USA), respectively, according to the manufacturer's instructions. The data were processed with FlowJo™ 10.6.1 software.

Cell invasion assay

Cell invasion assay was performed using a 24-well transwell chamber with Matrigel (356234, BD Pharmingen). After being starved in serum-free medium for 24 h, Huh7 cells were resuspended (1×10^5 cells in 200 μL of DMEM per well) in serum-free DMEM containing the indicated inhibitors and added to the upper chambers. The lower chambers were filled with 600 μL of DMEM containing 2% FBS with 1 or 10 ng/mL of HGF (100-39H, PeproTech) as chemoattractant and incubated at 37 °C for 48 h. Cells that migrated to the lower surface of chambers were fixed with methanol, stained with 0.5% crystal violet, and counted with a microscope (100×) (CTR6000, Leica). For hypoxia, cells were incubated at 5% CO_2 and 95% N_2 in a humidified incubator at 37 °C.

Colony formation assay

Cells at the logarithmic growth phase were seeded at a density of 1000 cells per well in 6-well plates and cultured with or without inhibitors for 10 days. Fresh medium was added every 3 days. The colonies were fixed with methanol and stained with 0.5% crystal violet. The blue colonies were counted on five randomly chosen fields under a microscope (100×) (CTR6000, Leica).

Wound healing assay

HUVECs were plated and allowed to confluence on marked plastic dishes. After washing with PBS buffer twice and being starved for 8 h in serum-free ECM medium, a wound gap in HUVEC monolayer was created by scratching with a 200-μL pipette tip. Cells were washed with PBS buffer and then cultured with or without drugs for 24 h. The wounds were monitored and photographed at 0 and 24 h. The healing was quantified by measuring the distance between edges.

Endothelial tubule formation assay

Matrigel (356234, BD Pharmingen) was plated in 24-well plates and allowed to solidify in a 37 °C cell culture incubator. HUVECs were resuspended in serum-free ECM medium with or without drugs, plated on Matrigel layer (1×10^5/mL), and incubated at 37 °C for 4 h. Tube networks were photographed using a phase-contrast microscope (DM IL LED, Leica). The angiogenic index was calculated as the number of branch points in a randomly selected visual field.

Lentivirus-mediated knockdown of gene expression

Short hairpin RNAs (shRNAs) targeting MET were cloned into pLKO.1-puro vector (Addgene). shRNA sequences are available in Table S1. For lentivirus generation, 1×10^7 293T cells were seeded in a 10-cm dish in DMEM supplemented with 10% FBS the day before transfection. Cells were transfected by changing to 10 mL of DMEM containing 20 μL of LipoFiter™ Liposomal Transfection Reagent (HB-TRLF, Hanbio) and 10 μg of pLKO.1-puro vector or pLKO shMET combined with 7.5 μg of psPAX2 and 2.5 μg of pMD2.G. After 6 h, the medium was changed with DMEM 10% FBS. After 48 h, the supernatant was collected, filtered with 0.45 mm filters, and used to infect HCC cell lines. The stable cell lines were obtained by puromycin selection for 1 week.

In vivo xenograft tumor model and immunohistochemistry (IHC)

Subcutaneous implantation models were established using Hepa1-6 cells. A total of 5×10^5 cells were resuspended in 80 μL of PBS and injected subcutaneously into the right side of the posterior flank of male C57BL/6 mice (4 weeks old, Shanghai Institute of Materia Medica, Chinese Academy of Sciences). After injection for 1 week and tumor volume reached about 100 mm^3, the mice were randomized into four groups: vehicle group (1.25% polyethylene glycol, 2.5% Tween-80, and 5% DMSO, orally, once every 2 days), cabozantinib group (30 mg/kg of cabozantinib in 1.25% polyethylene glycol, 2.5% Tween-80, and 5% DMSO, orally, once every 2 days), rapamycin group (2 mg/kg of rapamycin in 1.25% polyethylene glycol, 2.5% Tween-80, and 5% DMSO, orally, once every 2 days), and combination group (30 mg/kg of cabozantinib and 2 mg/kg of rapamycin in 1.25% polyethylene glycol, 2.5% Tween-80, and 5% DMSO, orally, once every 2 days). The volume of tumors was calculated by using the following formula: $a \times b^2/2$

(a and b refer to the largest and smallest diameter, respectively) every 3 days. After 2 weeks of treatment, the mice were sacrificed and tumors were collected.

Tumors were either homogenized in tumor lysis buffer for Western blot analysis or fixed with 4% formaldehyde solution and embedded in paraffin. Sections were deparaffinized and rehydrated in alcohol gradient, and subjected to microwave antigen retrieval. Sections were treated with 0.3% hydrogen peroxide to block the endogenous peroxidase. After blocking with 2% BSA for 1 h at RT, sections were incubated with primary antibodies and secondary antibodies following the manufacturer's instructions. Color development was performed with HRP (DAB Peroxidase Substrate Kit (Vector Laboratories, SK-4100)).

The primary antibodies used for IHC included cMet (8198, Cell Signaling Technology), CD31 (77699, Cell Signaling Technology), cyclin D1 (ab134175, Abcam), PCNA (13110, Cell Signaling Technology), pmTOR (Ser2448) (ab109268, Abcam), and pAKT (Ser473) (ab81283, Abcam). The secondary antibodies used for IHC include Peroxidase AffiniPure Goat Anti-Rabbit IgG (H + L) (111-035-003, JACKSON).

In vivo lung metastasis model

Lung metastasis models were established by intravenously injecting Hepa1-6 cells. Briefly, 2×10^6 cells were resuspended in 100 μL of PBS and injected into the tail vein of male C57BL/6 mice (4 weeks old, Shanghai JieSijie Laboratory Animals Co., Ltd.). After injection for 2 weeks, the mice were randomized into four groups: vehicle group (1.25% polyethylene glycol, 2.5% Tween-80, and 5% DMSO, orally, once every 2 days), cabozantinib group (30 mg/kg of cabozantinib in 1.25% polyethylene glycol, 2.5% Tween-80, and 5% DMSO, orally, once every 2 days), rapamycin group (2 mg/kg of rapamycin in 1.25% polyethylene glycol, 2.5% Tween-80, and 5% DMSO, orally, once every 2 days), and combination group (30 mg/kg of cabozantinib and 2 mg/kg of rapamycin in 1.25% polyethylene glycol, 2.5% Tween-80, and 5% DMSO, orally, once every 2 days). Mice were sacrificed after 2 weeks of treatment. The lungs were removed, fixed in paraformaldehyde (4%), and embedded in paraffin. Consecutive sections were made for every lung tissue block and stained with hematoxylin and eosin (HE). The number of lung metastases in the maximal section of the metastatic lesion was calculated and evaluated.

Statistical analysis

All data are presented as mean ± SD as indicated in the figure legends. Statistical analysis was performed with SPSS10.0 software. Depending on the data, Student's *t*-test and one- or two-way ANOVA were used to analyze quantitative variables. Differences were considered statistically significant at $P < 0.05$.

Results

cMet-low HCC cells are resistant to cMet inhibitors

Consistent with our previous report that *MET* amplification and cMet overexpression were positively associated with the sensitivity of HCC cells to cMet inhibitors [12], low concentration (2 μmol/L) of cabozantinib showed no obvious inhibitory effect on the phosphorylation of cMet and expression of cyclin D1 and cleaved-PARP in Huh7 cells with low cMet expression (Fig. 1A). We then assessed the responses of different HCC cells to cMet inhibitors, cabozantinib, and NZ001. NZ001 is a novel dual cMet and VEGFR2 inhibitor. MHCC-97H and MHCC-97L cells, which had high cMet expression, were more sensitive to cabozantinib and NZ001 than HCC cells with low cMet expression (Fig. 1B). The cell growth curves were similar among HCC cells treated with cabozantinib and NZ001 (Fig. 1B), indicating their similar direct inhibitory effects on HCC cells. Therefore, NZ001 was used to verify the result of cabozantinib in this study. Moreover, we retrieved the Genomics of Drug Sensitivity in Cancer database for more drug response data about cabozantinib on HCC cells. We found that cells with IC50 > 5 μmol/L were identified as resistant to cabozantinib, and 13 out of 17 cell lines screened were cabozantinib-resistant (Fig. 1C). Then, we analyzed cMet expression in 10 human HCC tissues by IHC staining and found that cMet expression exhibited extensive heterogeneity among different regions within the same HCC tissues (Fig. 1D). This molecular trait reflects different sensitivity of distinct colonies in HCC to cMet inhibitors. Collectively, these results indicate that a spatial heterogeneity of cMet expression exists in HCC tissues and that cMet-low HCC cells show primary resistance to cMet inhibitors.

Rapamycin increases the sensitivity of cMet inhibitor-resistant HCC cells to cabozantinib

As RTKs are the main targets for cabozantinib, we next examined the activations of RTKs in three cMet inhibitor-resistant HCC cell lines and observed the diverse expression of activated RTK signaling pathways (Fig. S1). Moreover, cabozantinib treatment did not affect the phosphorylation of these RTKs (Fig. S1). Therefore, we hypothesized that the inhibition of common and key downstream signal molecules of RTKs could be an alternative to cover as many cMet inhibitor-resistant HCC cells as possible. We examined the inhibitory effect of cabozantinib in combination with inhibitors targeting the key points of MAPK–ERK and PI3K–AKT–mTOR cascades on cMet inhibitor-resistant Huh7 and PLC cells

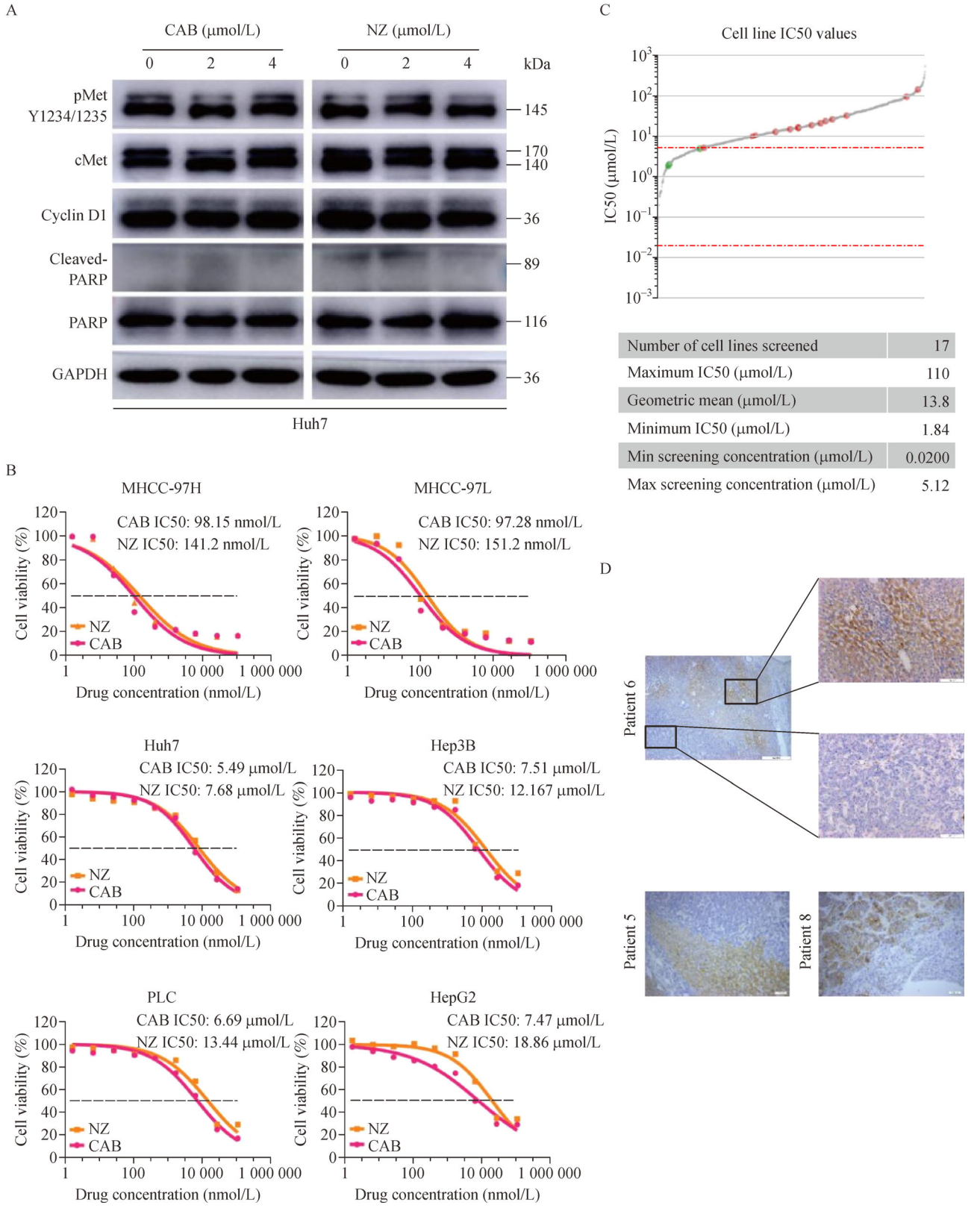

Fig. 1 Low expression of cMet is correlated with poor response of HCC cells to cabozantinib. (A) The expression of cMet, pMet (Y1234/1235), cyclin D1, and cleaved-PARP levels in Huh7 cells treated with cabozantinib (CAB, 2 or 4 μmol/L) or NZ001 (NZ, 2 or 4 μmol/L) was determined by Western blot analysis. (B) Cell survival curves of a panel of HCC cell lines treated with cabozantinib (CAB) or NZ001 (NZ) for 3 days were detected by CCK8 assay, and the IC50 values of cabozantinib and NZ001 are shown. (C) Drug response data (IC50) of HCC cell lines to cabozantinib in the Genomics of Drug Sensitivity in Cancer database are shown. (D) Representative images of IHC staining of cMet in 10 HCC samples. For patient 6, the areas labeled with black boxes in the left panel are shown in the right panels with higher magnification. Bar of left panel, 500 μm. Bar of right panels, 100 μm. For patients 5 and 8, bar, 200 μm. Data are shown as the mean ± SD from three independent biological replicates.

using cell proliferation assay. We found that, in combination with cabozantinib, mTOR inhibitor rapamycin exhibited the most effective inhibition of Huh7 and PLC cell proliferation (Fig. 2A). We further expanded the combination treatment screening to the common target drugs, and the inhibitory efficiency of these drugs varied between Huh7 and PLC cells. The EGFR inhibitor gefitinib and Wee1 inhibitor MK-1775 could notably enhance the anti-proliferation effect of cabozantinib on PLC cells but only showed modest inhibition on Huh7 cells, which was consistent with the diverse expression of activated RTKs among cMet inhibitor-resistant HCC cells (Fig. S1). Moreover, among the three cMet-low HCC cell lines we examined, mTOR signals were all activated, which could not be effectively inhibited by cabozantinib (Fig. S1). The effectiveness of small molecular inhibitors was confirmed by examining the phosphorylation of molecular targets (Fig. 2B–2E). These results indicate that cabozantinib in combination with rapamycin is a potential choice for treating cMet inhibitor-resistant HCC.

Combination of rapamycin and cabozantinib shows synergistic inhibition of cMet inhibitor-resistant HCC cell proliferation

To further evaluate the effect of cabozantinib and rapamycin combination on cMet inhibitor-resistant HCC cells, we performed cell proliferation assay and calculated their CI value in Huh7 and PLC cells. Rapamycin alone showed only moderate inhibition on cell growth. The cell survival percentage of Huh7 and PLC cells was 50%–60% and around 50%, respectively, when the rapamycin concentration reached 2 μmol/L or more (Fig. 3A and 3B). However, the inhibitory effect of cabozantinib or NZ001 on HCC cell growth increased in a dose-dependent manner (Fig. 3A and 3B). The combination of cabozantinib and rapamycin synergistically inhibited cell growth (Fig. 3A and 3B), with CI values less than one at all concentrations examined (Fig. 3C and 3D). Similar synergistic inhibitory effect was also observed in the combination of NZ001 with rapamycin (Fig. 3A–3D). We further found that the colony formation ability of Huh7 and PLC cells treated with cabozantinib and rapamycin was much lower than that of HCC cells treated with each inhibitor alone (Fig. 3E and 3F). Moreover, to evaluate the anti-tumor effects of cabozantinib and rapamycin on HCC cells with high cMet expression when cMet was knocked down, we generated two MET-specific shRNAs to silence cMet expression (shMET). The shMET#1 induced more significant knockdown effects than the other in MHCC-97H cells that highly expressed cMet, and was adopted for knocking down cMet expression (Fig. S2A). We performed cell proliferation assay of shNC and shMET MHCC-97H treated with cabozantinib and rapamycin and found that the inhibitory effect on shMET MHCC-97H was compromised compared with shNC MHCC-97H (Fig. S2B). The underlying mechanism was that because cMet overexpression was positively associated with the sensitivity of HCC cells to cMet inhibitors (Fig. 1B), knocking down cMet expression in MHCC-97H with high cMet expression allowed them to acquire resistance to cMet inhibitors. Collectively, these data indicated a synergistic interaction between cabozantinib and rapamycin in inhibiting cMet inhibitor-resistant HCC cells growth *in vitro*.

Rapamycin enhances the inhibitory effect of cabozantinib on angiogenesis

On the basis of the known anti-angiogenic function of rapamycin and VEGFR2 inhibitor, we determined whether cabozantinib and rapamycin have synergistic anti-angiogenesis effect. Cabozantinib or rapamycin alone suppressed the migration ability of HUVECs, and this effect was significantly enhanced by combination treatment of rapamycin and cabozantinib or NZ001 (Fig. 4A and 4B). In addition, we analyzed the angiogenic index measured by tubule formation assay. Similarly, combination treatment induced the most remarkable inhibition of tubule formation. The angiogenic index in the combination treatment group was significantly smaller than that of the cabozantinib, NZ001, or rapamycin alone group (Fig. 4C and 4D). To further validate the anti-angiogenesis effect of combination treatment *in vivo*, we detected CD31-positive blood vessels in the subcutaneous implantation models of Fig. 6A by IHC staining. Compared with vehicle, cabozantinib and rapamycin alone significantly reduced the blood vessel density of tumor tissues. Furthermore, the anti-angiogenesis effect of combination treatment was greater than that of each single agent alone (Fig. 4E and 4F). These data indicate the enhanced anti-angiogenesis effect of combination treatment of cabozantinib and rapamycin.

Rapamycin augments the inhibitory effect of cabozantinib on the metastasis of HCC cells

Our previous study indicated that hypoxia induced by VEGFR blockade could increase HCC cell invasion induced by HGF [12]. We detected the invasion ability of HCC cells treated with 1 or 10 ng/mL of HGF under normoxia or hypoxia condition. We found that 1 ng/mL of HGF slightly enhanced the invasion of Huh7 cells under normoxia condition, and the number of invading cells increased when treated with 10 ng/mL of HGF (Fig. 5A and 5C). Consistent with our previous findings, hypoxia augmented the sensitivity of HCC cells to HGF, as indicated by the significantly enhanced invasion of HCC cells treated with the same level of HGF under hypoxia condition (Fig. 5A and 5C). We further determined whether rapamycin augmented the inhibitory effect of

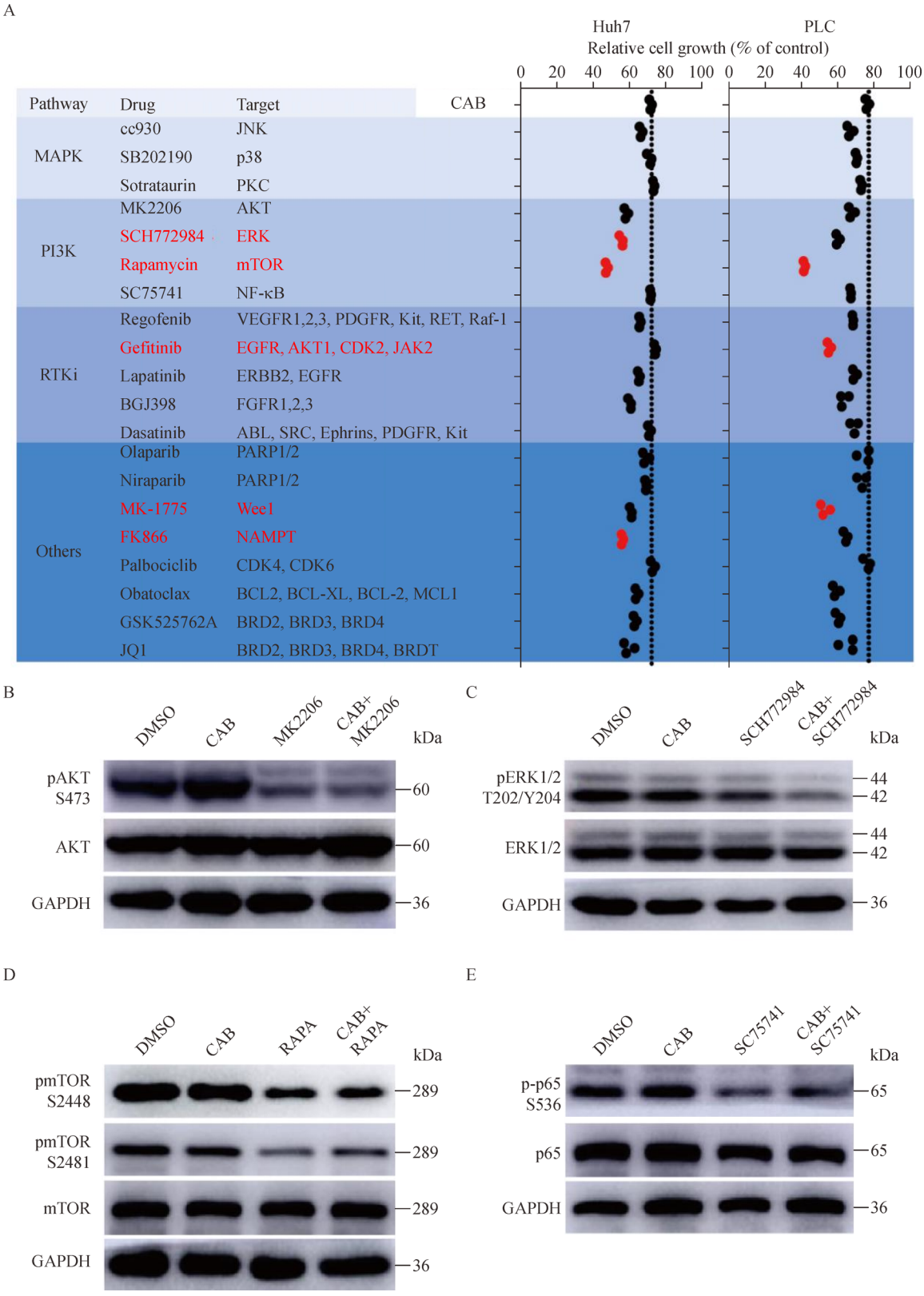

Fig. 2 Rapamycin can be used in combination with cabozantinib to inhibit the proliferation of cMet inhibitor-resistant HCC cells. (A) Percentage of living Huh7 and PLC cells after treatment with cabozantinib (CAB) alone or in combination with a panel of inhibitors for 3 days. The relative cell number of the control group was set as 100%; the three most effective inhibitors are marked in red. The significance was determined by one-way ANOVA (Bonferroni post test). (B–E) The phosphorylation levels of AKT (S473) (B), ERK (T202/Y204) (C), mTOR (S2448 and S2481) (D), and p65 (S536) (E) in Huh7 cells treated with the indicated inhibitors (MK2206 (AKTi), SCH772984 (ERKi), rapamycin (RAPA) (mTORi), and SC75741 (p65i)) or in combination with cabozantinib (CAB) were determined by Western blot analysis. Representative images from three independent experiments are shown.

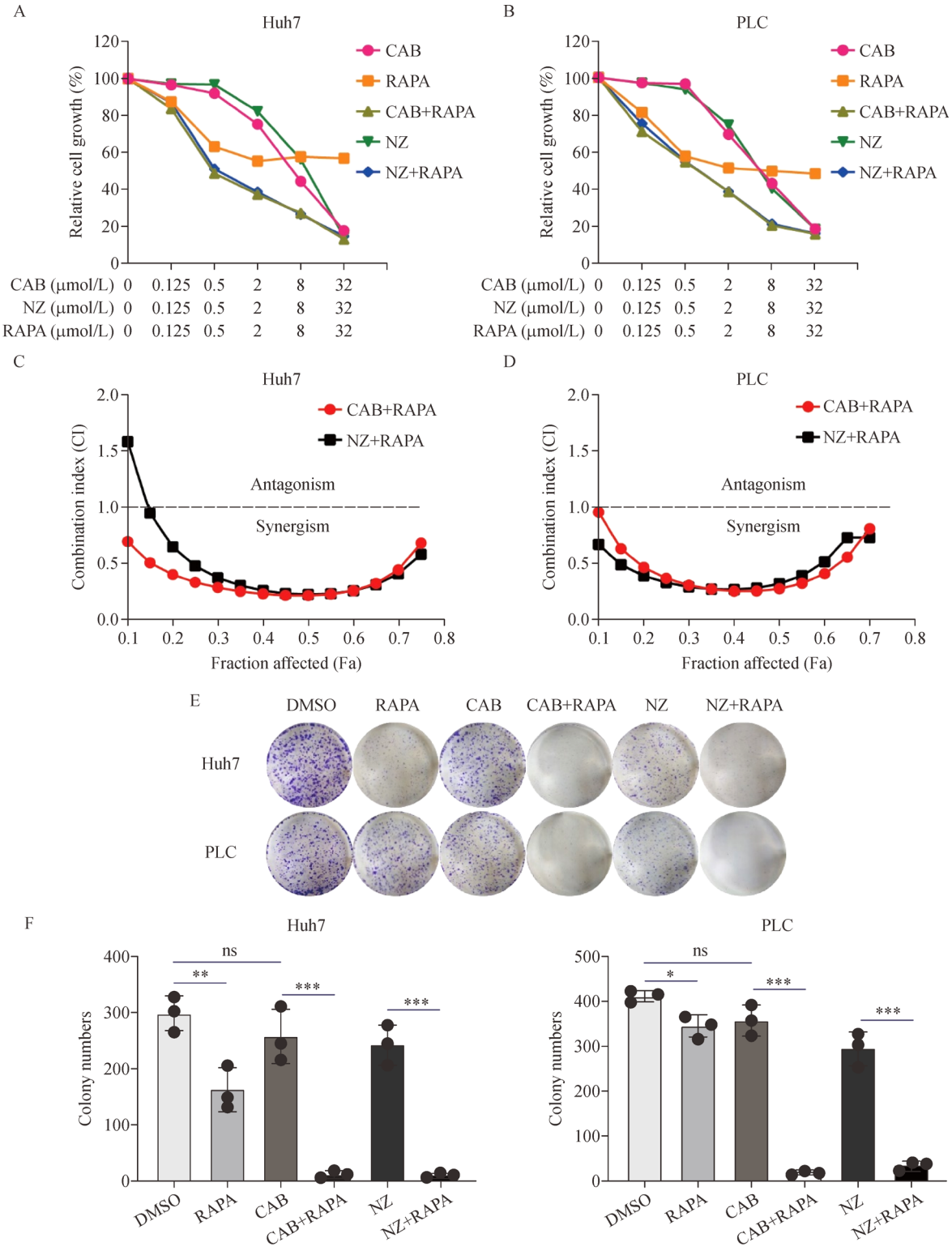

Fig. 3 Rapamycin sensitizes cMet-low HCC cells to cabozantinib. (A, B) The proliferation of Huh7 (A) and PLC (B) cells treated with cMet inhibitor (cabozantinib (CAB) or NZ001 (NZ)) and rapamycin (RAPA) alone or in combination at the indicated concentration for 3 days was measured using CCK8 assay. The significance was determined by two-way ANOVA (Bonferroni post test). (C, D) The CI of rapamycin (RAPA) and cMet inhibitor (cabozantinib (CAB) or NZ001 (NZ)) in inhibiting the proliferation of Huh7 (C) and PLC (D) cells was calculated using the Chou–Talalay method. (E, F) Colony formation assay of Huh7 and PLC cells treated with cMet inhibitor (cabozantinib (CAB, 2 μmol/L) or NZ001 (NZ, 2 μmol/L)) and rapamycin (RAPA, 10 nmol/L) alone or in combination for 14 days. Representative images (E) and bar charts of the colony numbers (F) are shown. For (F), the significance was determined by one-way ANOVA (Bonferroni post test). Data are shown as the mean ± SD from three independent biological replicates. $^{*}P < 0.05$; $^{**}P < 0.01$; $^{***}P < 0.001$; ns: not significant.

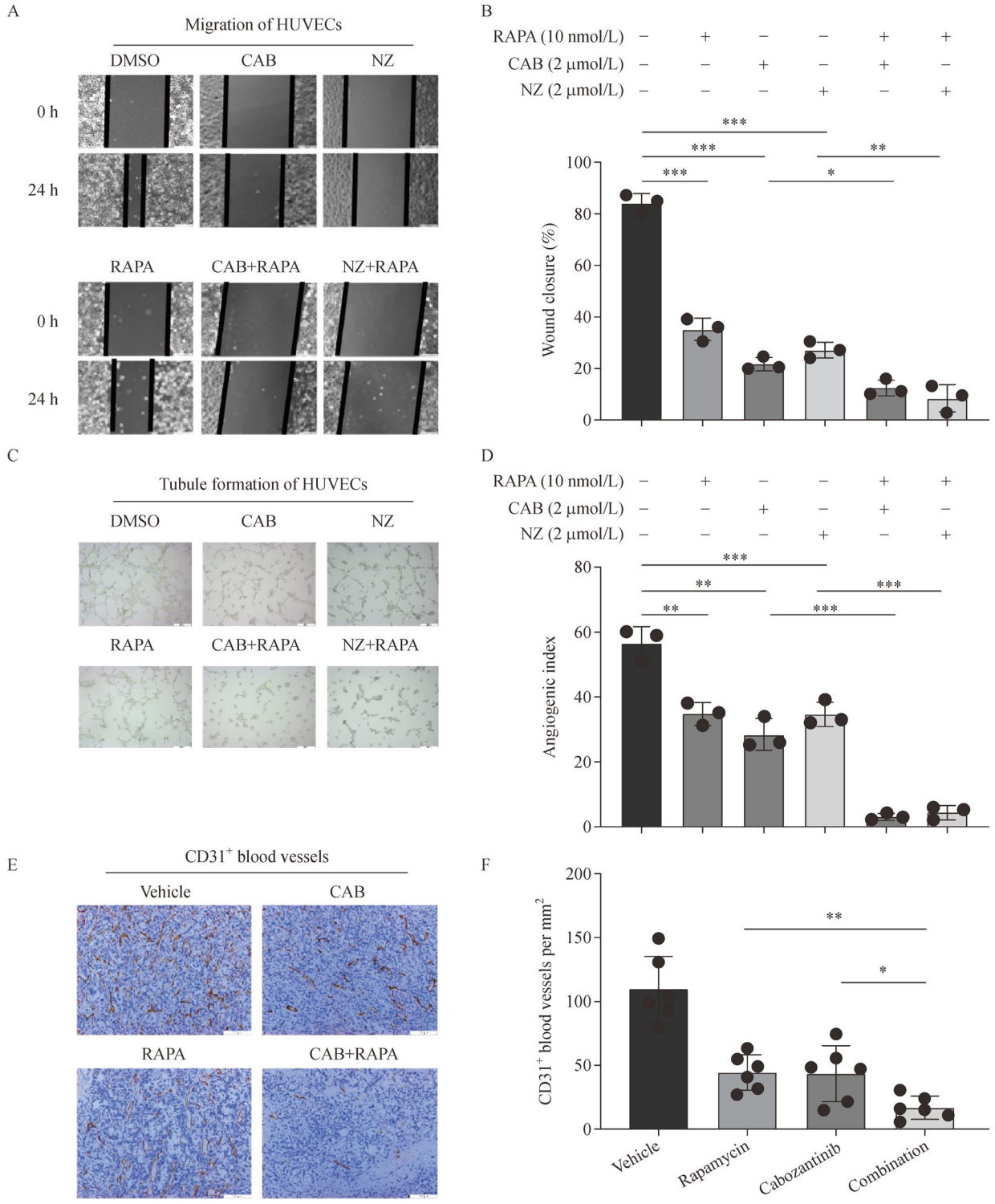

Fig. 4 The combination treatment of cabozantinib and rapamycin shows enhanced anti-angiogenesis effect. (A, B) In the migration assay, 2 μmol/L of cabozantinib (CAB), 2 μmol/L of NZ001 (NZ), and 10 nmol/L of rapamycin (RAPA) alone or in combination were used to treat HUVECs. The representative images of scratches after 0 and 24 h (A) and the percentage of wound healing 24 h after scratching are shown (B). Bar, 200 μm. Data are shown as the mean ± SD from three independent biological replicates. (C, D) Tubule formation assay of HUVECs treated with 2 μmol/L of cabozantinib (CAB), 2 μmol/L of NZ001 (NZ), and 10 nmol/L of rapamycin (RAPA) alone or in combination for 4 h. Representative images are shown (C), and the angiogenic index was calculated (D). Bar, 200 μm. Data are shown as the mean ± SD from three independent biological replicates. (E, F) CD31 expression of subcutaneous implantation tumors from C57BL/6 mice treated with indicated inhibitors was detected by IHC staining. The representative images are shown (E), and $CD31^+$ blood vessels per mm^2 were calculated accordingly ($n = 6$) (F). Bar, 100 μm. Data are shown as the mean ± SD from six independent biological replicates. For (B), (D), and (F), the statistical significance was determined by one-way ANOVA (Bonferroni post test). *$P < 0.05$, **$P < 0.01$, ***$P < 0.001$.

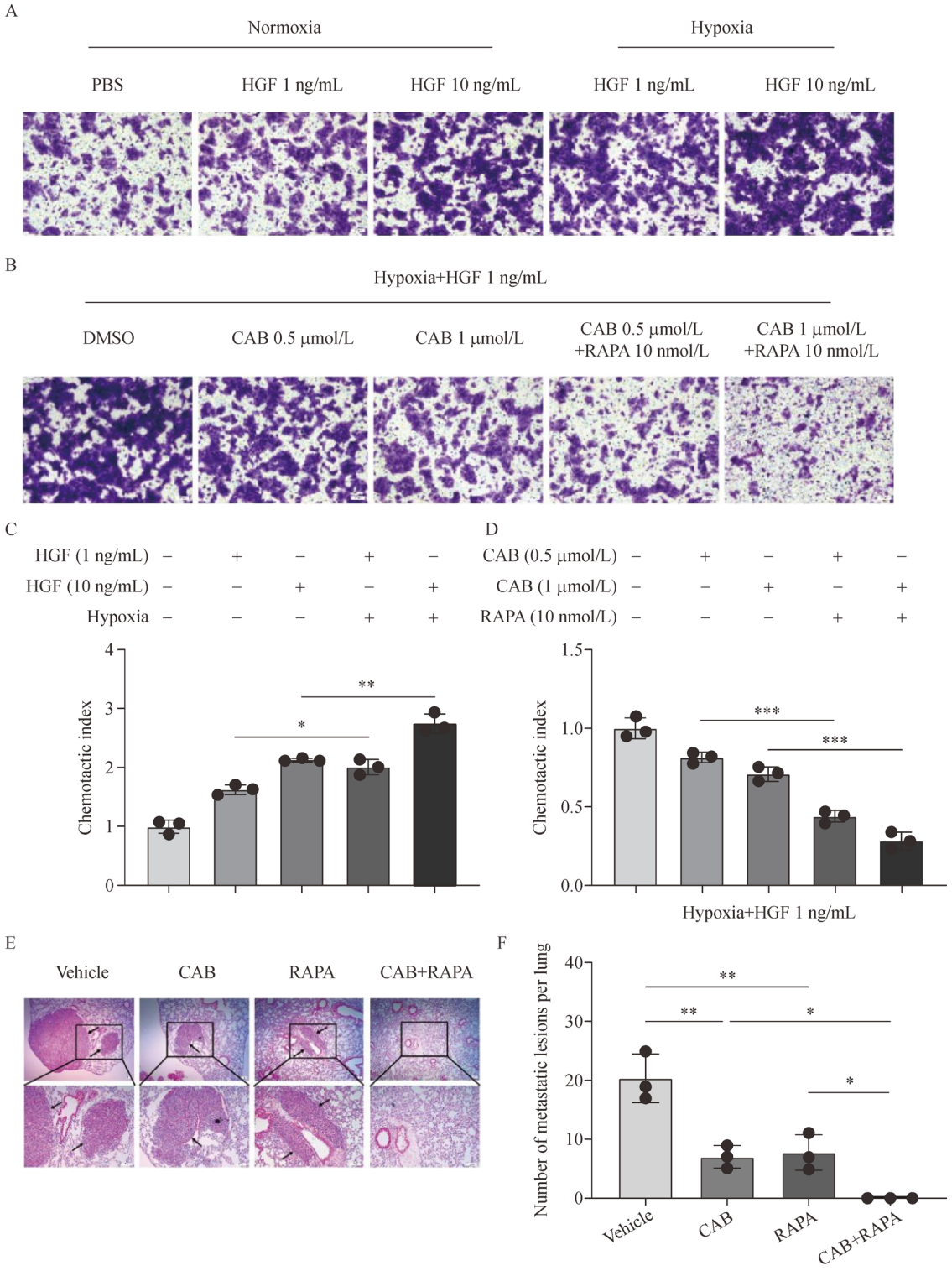

Fig. 5 Combination treatment results in stronger inhibition of HGF-induced cell invasion of Huh7 cells under hypoxia condition. (A, C) Invasion assay of Huh7 cells treated with 1 or 10 ng/mL of HGF under normoxia or hypoxia condition for 48 h. The representative images are shown (A), and the chemotactic index was calculated as the ratio of the cell number of treatment groups to that of the control group (C). Bar, 100 μm. (B, D) The inhibitory effects of cabozantinib (CAB, 0.5 μmol/L and 1 μmol/L) alone or combined with rapamycin (RAPA, 10 nmol/L) on the invasion ability of Huh7 cells treated with 1 ng/mL of HGF under hypoxia condition were measured (B), and the chemotactic index was calculated (D). Bar, 100 μm. Data are shown as the mean ± SD from three independent biological replicates. For (C) and (D), the statistical significance was determined by one-way ANOVA (Bonferroni post test). (E, F) The effects of rapamycin (RAPA) and cabozantinib (CAB) alone or in combination on tumor metastasis in lung metastasis models. The representative HE staining images of lung tissues (E) and the average numbers of lung metastatic lesions (F) from three mice per group are shown. Arrows indicate lung metastatic lesions, and the areas labeled with a black box in the upper panel are shown in the lower panel with higher magnification. Scale bar, 100 μm. For (F), data are shown as the mean ± SD ($n = 3$), and the significance was determined by one-way ANOVA (Bonferroni post test). *$P < 0.05$, **$P < 0.01$, ***$P < 0.001$.

cabozantinib on HGF-induced Huh7 invasion under hypoxia condition using the chemotactic index, and the results suggested that the chemotactic index of Huh7 cells with combination treatment was significantly less than that of HCC cells treated with cabozantinib alone. Moreover, the inhibitory effect of combination treatment on HGF-induced invasion of Huh7 cells notably increased dose-dependently (Fig. 5B and 5D). Finally, to evaluate the combined effects on the metastasis of HCC *in vivo,* we injected Hepa1-6 cells into the tail vein of male C57BL/6 mice to establish a lung metastasis model. After 2 weeks, vehicle, cabozantinib, rapamycin, and combined drugs were administered for another 2 weeks. Then, mice were sacrificed, and their lungs were removed, sliced, and stained with HE to evaluate lung metastasis. We found that compared with the vehicle group, a remarkable decrease in the number of lung metastatic lesions was observed in other groups, and no lung metastasis lesion was found in C57BL/6 mice under the combination treatment of cabozantinib and rapamycin (Fig. 5E and 5F). These data indicate that combination treatment of cabozantinib and rapamycin exhibits more effective suppressive effect on the metastasis of HCC cells than cabozantinib alone.

Anti-tumor effects of combination treatment on the growth of HCC xenograft *in vivo*

The synergistic effects of cabozantinib in combination with rapamycin were further confirmed in immunocompetent subcutaneous tumor model. In our previous work, Hepa1-6 was identified as a cMet-low murine HCC cell line that was insensitive to cMet inhibitor [12]. We first detected the inhibitory effect of combination treatment on the proliferation and colony formation of Hepa1-6 cells *in vitro*. Similar to the studies above, cMet inhibitors (cabozantinib, NZ001, and PF04217903) or rapamycin alone showed no inhibitory effect, whereas the synergistic effects of combination treatment on inhibiting proliferation and colony formation were observed in Hepa1-6 cells (Fig. S3A and S3B). Next, vehicle, cabozantinib, rapamycin, and combined drugs were administered to C57BL/6 mice 1 week after the establishment of the subcutaneous tumor model of Hepa1-6 cells (tumor volume reached about 100 mm^3). We found that compared with vehicle, all other treatments delayed tumor growth significantly, among which combination treatment exerted the most effective inhibitory effect (Fig. 6A–6C). In addition, no significant weight loss was observed among all groups, which indicated that the combination treatment of cabozantinib and rapamycin did not significantly increase toxicity and could be well tolerated (Fig. 6D). To determine whether the cell cycle is affected by combination treatment, we examined the cyclin D1 expression in subcutaneous transplantation tumors by IHC staining. A modest decrease of cyclin D1 in the cabozantinib treatment group and a significant decrease in rapamycin-treated tumors were observed, while the combination of cabozantinib and rapamycin resulted in a much more obvious decrease of cyclin D1 expression than the other treatments (Fig. 6E and 6F). In addition, we used PCNA, another indicator of cell proliferation, to validate the effect of combination treatment on cell proliferation. We found that the proliferation index decreased using each inhibitor alone, and the biggest decrease occurred in the combination treatment group (Fig. 6E and 6G). Finally, to assess whether combination therapy suppressed AKT/mTOR signaling, we examined pmTOR and pAKT expression in subcutaneous xenograft by IHC staining. Cabozantinib alone failed to suppress the phosphorylation of mTOR, which could be inhibited by rapamycin alone. Conversely, rapamycin led to feedback activation of AKT, which could be attenuated by cabozantinib. The suppression of pmTOR and pAKT was achieved only in the combination of cabozantinib and rapamycin (Fig. 6E, 6H, and 6I). Taken together, our *in vivo* results reveal that rapamycin augments the anti-tumor effects of cabozantinib on the growth of cMet inhibitor-resistant HCC.

Combination treatment inhibits the phosphorylation of AKT, mTOR, and ERK and induces cell cycle arrest

We next investigated the mechanism underlying the synergetic inhibitory effects of the combination treatment. Cabozantinib and NZ001 alone failed to inhibit the phosphorylation of AKT, ERK, and mTOR, the core signal molecules of RTK downstream pathways, in cMet inhibitor-resistant Huh7 cells (Fig. 7A). By contrast, rapamycin suppressed the phosphorylation of mTOR, p70S6K, and ERK but led to feedback activation of AKT and slightly enhanced cMet phosphorylation, which could be attenuated by cabozantinib and NZ001 (Fig. 7A). Therefore, the combination treatment could block the PI3K–AKT–mTOR and MAPK–ERK pathways downstream of RTKs at the same time. Considering that the PI3K–AKT–mTOR and MAPK–ERK pathways play a role in cell cycle regulation, we detected the expression of cyclin D1, a critical regulator of G1–S phase transition, and investigated cell cycle by flow cytometry. The results indicated that cabozantinib, NZ001, or rapamycin alone showed no effect on cell cycle, while the combination treatment induced a significant downregulation of cyclin D1 and an obvious cell cycle arrest compared with the control group (G1%: 50.65 or 52.71 vs. 34.31, $P < 0.001$) (Fig. 7B–7D). Moreover, we detected the cleaved-PARP level, an indicator of apoptosis, and conducted annexin V-FITC/PI apoptosis assay using flow cytometry after treatment with inhibitors alone or in combination. The results showed no obvious cleaved-PARP alteration or changes in the percentage of apoptotic Huh7 cells treated with single drug or combined drugs (Fig. S4A–S4C).

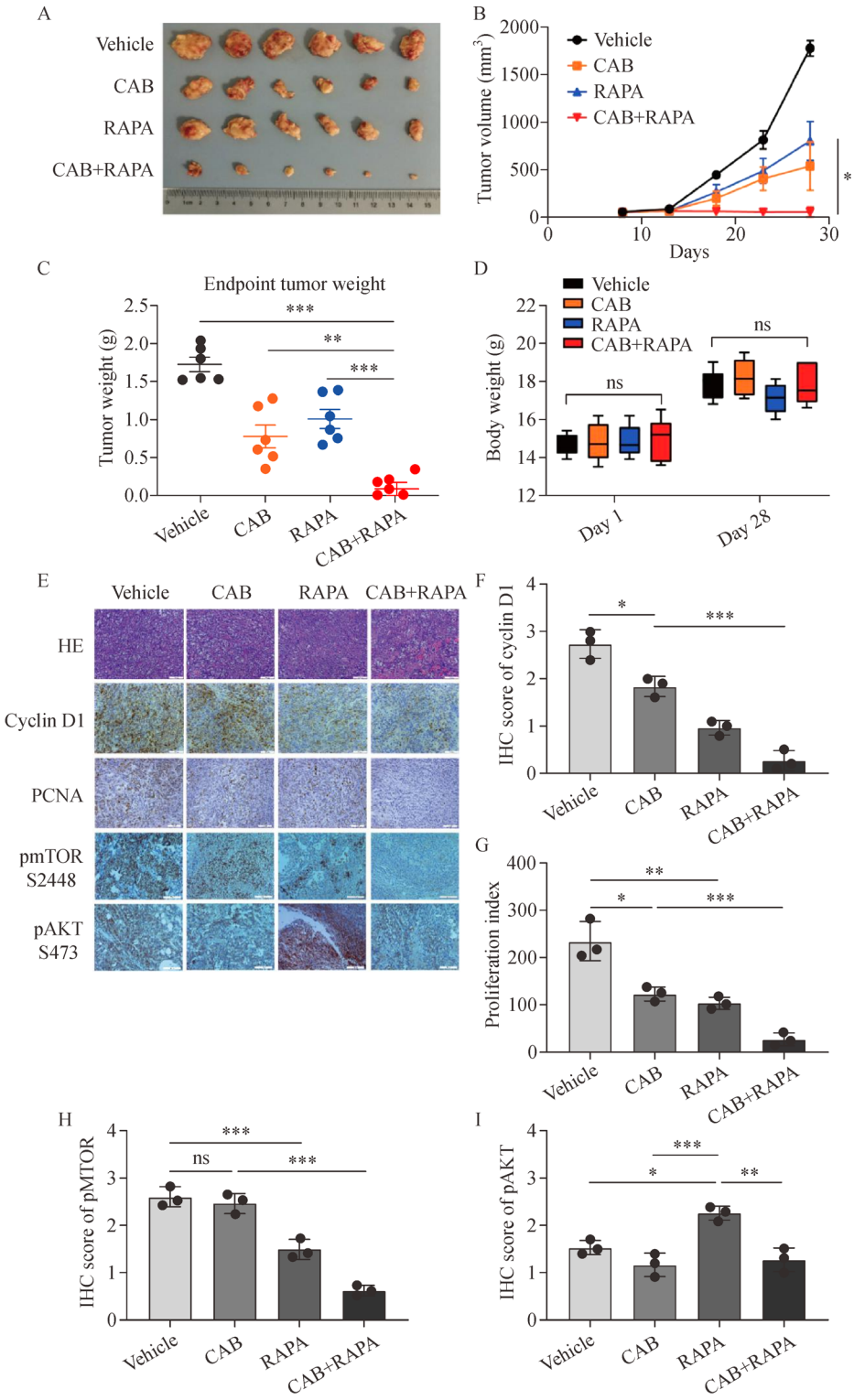

Fig. 6 Rapamycin augments the inhibitory effect of cabozantinib on the tumor growth of HCC xenograft *in vivo*. (A–C) Effects of rapamycin (RAPA) and cabozantinib (CAB) alone or in combination on tumor growth in subcutaneous xenograft models. Photos (A), tumor volume (B), and endpoint tumor weight (C) are shown. For (B) and (C), data are shown as mean ± SD ($n = 6$). The significance was determined by two-way ANOVA (Bonferroni post test) (B) and one-way ANOVA (Bonferroni post test) (C). (D) The body weight of mice from different groups at day 1 (subcutaneous injection) and day 28 (mice sacrificed) was measured. Data are shown as mean ± SD ($n = 6$). The significance was determined by one-way ANOVA (Bonferroni post test). (E–I) The expression of cyclin D1, PCNA, pmTOR (S2448), and pAKT (S473) in tumors from different experimental groups treated with the indicated inhibitors was detected by IHC staining. The representative images are shown (E). The IHC score of cyclin D1 (F), proliferation index based on the IHC score of PCNA (G), IHC score of pmTOR (S2448) (H), and IHC score of pAKT (S473) (I) are shown. Bar, 100 μm. HE, hematoxylin and eosin. For (F–I), data are shown as the mean ± SD ($n = 3$), and the significance was determined by one-way ANOVA (Bonferroni post test). *$P < 0.05$, **$P < 0.01$, ***$P < 0.001$; ns, not significant.

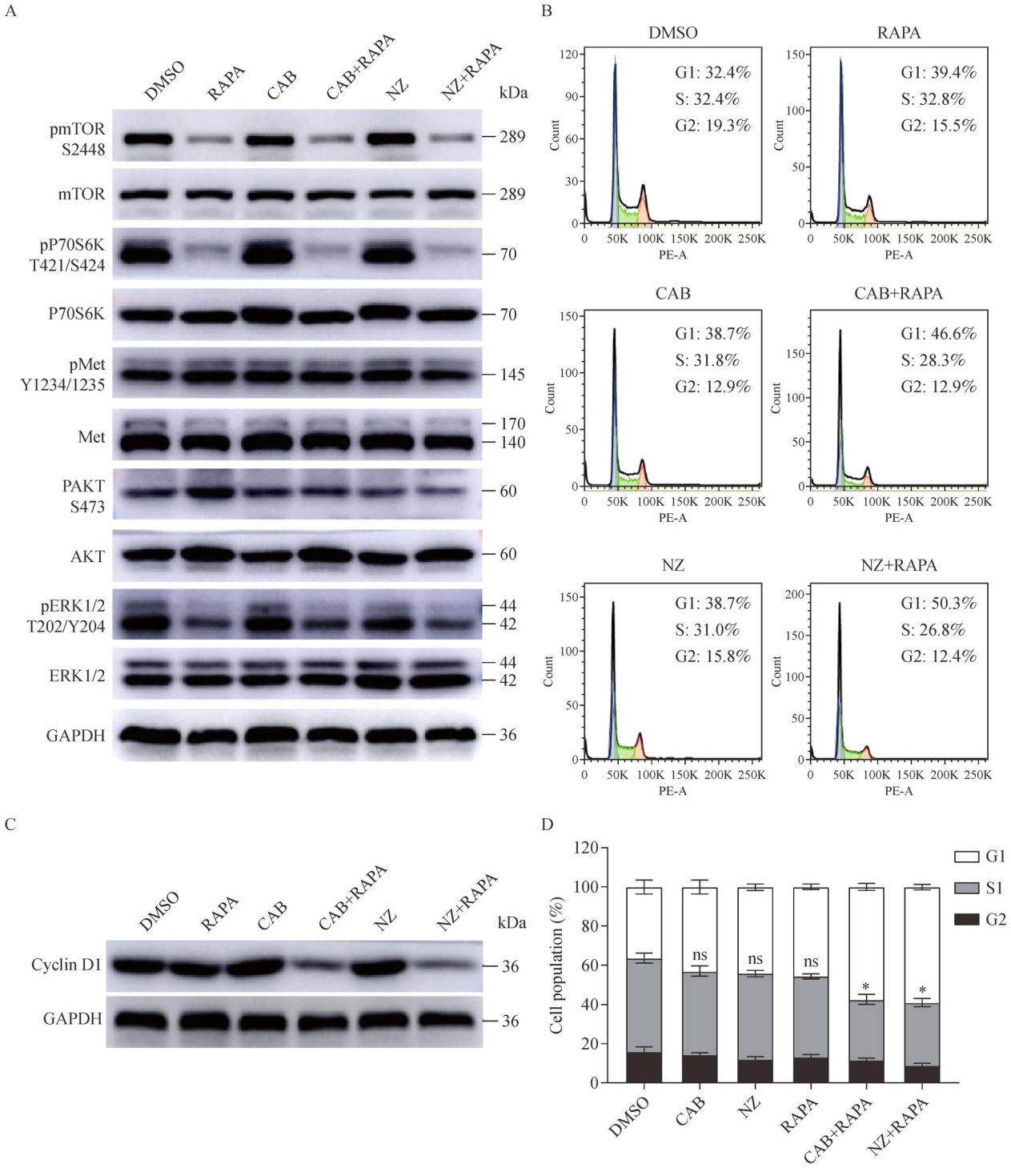

Fig. 7 Combination treatment of cabozantinib and rapamycin leads to the suppression of RTK signaling downstream effectors and cell cycle arrest. (A, C) The inhibitory effect of cMet inhibitor (cabozantinib (CAB) or NZ001 (NZ)) and rapamycin (RAPA) alone or in combination on the phosphorylation of cMet (Y1234/1235) and downstream effectors AKT (S473), ERK (T202/Y204), mTOR (S2448), and P70S6K (T421/S424) (A) and on the expression of cyclin D1 (C) in Huh7 cells was analyzed by Western blot. (B, D) Huh7 cells treated with cMet inhibitor (cabozantinib (CAB) or NZ001 (NZ), 2 μmol/L) and rapamycin (RAPA, 10 nmol/L) alone or in combination were subjected to PI staining and assessed by flow cytometry (B). The percentage of Huh7 cells in each cell cycle stage was calculated (D). For (D), the statistical significance was determined by one-way ANOVA (Bonferroni post test). Data are shown as the mean ± SD from three independent biological replicates. *$P < 0.05$; ns, not significant.

These studies indicate that combination treatment synergistically inhibits the phosphorylation of AKT, mTOR, and ERK and induces cell cycle arrest in cMet inhibitor-resistant HCC cells.

Discussion

The cMet signaling pathway has been implicated in HCC progression, including proliferation, invasion, and hypoxia resistance [14]. Elevated expressions of cMet and its ligand HGF have been proved to indicate poor prognosis in HCC patients [15,16]. Our previous results indicated that cMet-low HCC cell lines (Huh7, PLC, HepG2, Hepa1-6) were relatively resistant to cabozantinib treatment compared with cMet-high HCC cell lines (MHCC-97H and MHCC-97L), with oral administration of cMet inhibitor leading to more tumor growth inhibition of MHCC-97H xenografts than Huh7 xenografts [12]. Nevertheless, several clinical trials have indicated that the IHC score of cMet expression or *MET* gene amplification showed limited power to predict the response of advanced-stage HCC patients to cMet inhibitors [17].

HCC harbors remarkable spatial heterogeneity—an individual tumor might comprise diverse cancer cells with distinct molecular driver alterations, thus providing the fuel for drug resistance and relapse [18,19]. Herein, we found a remarkable heterogeneity of cMet expression among distinct regions within the same HCC tumor tissue. On the basis of our previous data showing that the level of cMet expression or *MET* amplification of HCC cell lines was correlated with the sensitivity to cMet inhibitors [12], we hypothesized that under selection pressure, cMet-high HCC cells that are sensitive to cMet inhibitors are obliterated, while HCC cells with low cMet expression survive and evolve more progressively. In other words, the heterogeneity of cMet expression within HCC tumor tissue mediates the primary resistance of HCC to cMet inhibitors. Moreover, we found the primary resistance of a majority of HCC cell lines to cMet inhibitors *in vitro* in this study and the low ratio of cMet expression in HCC samples previously reported [12]. On this basis, we proposed a combination strategy to target cMet inhibitor-resistant HCC cells in this study.

The targeted drugs proved to improve the prognosis of HCC patients mainly targeted RTKs [7]. One of the approaches to reduce the primary resistance is to combine with other RTK inhibitors on the basis of the IHC-staining-detected abnormal activation of RTK signaling [20,21]. However, it is unfeasible to cover all the abnormally activated RTKs detected at the same time. On one hand, the activated RTK signaling pathways in cMet inhibitor-resistant HCC cells are diverse [22]. On the other hand, it is hard to obtain clinical tissue biopsy of unresectable HCC patients. Thus, cMet inhibitors combined with small molecular inhibitors targeting common and druggable molecules downstream of RTK signaling pathways may be a rational alternative [23–25]. In this regard, we screened inhibitors targeting these main downstream proteins listed in Fig. 2A. Herein, our results indicated that the combination of cabozantinib and rapamycin, a specific inhibitor of mTOR, synergistically led to significantly enhanced inhibition of cMet inhibitor-resistant HCC cells in terms of proliferation, colony formation, cell cycle regulation, invasion, and angiogenesis.

mTOR is an essential integrator of growth factor-activated pathways to regulate various functions, including cell proliferation, survival, and metabolism [7]. mTORC1 is mainly activated through the phosphoinositide 3-kinase (PI3K)/AKT signaling pathway [26,27]. mTOR inhibitors have been investigated in cancer treatment for decades and were tested in several ongoing clinical trials for patients with advanced HCC. A previous study revealed that the mTOR signaling pathway was abnormally activated in nearly half of HCC tissues, and the inhibition of mTOR could extend the survival of mice harboring HCC xenograft tumors [28]. However, the efficiency of mTOR inhibitors could be impaired by the feedback activation of AKT, which provided survival signal to cancer cells. Our results indicated that this side effect could be attenuated by cabozantinib, which was in line with a previous report in epithelioid sarcoma showing that AKT activation induced by mTOR inhibition was dependent on the HGF–cMet signaling pathway [29]. For cMet inhibitor-resistant HCC cells, rapamycin could in turn inhibit mTOR signaling and ERK phosphorylation, which are core intermediate molecules of RTK signaling transduction pathways. These results could account for the synergistic effects of combination treatment *in vitro*.

Apart from its direct anti-tumor activity, cabozantinib also suppresses angiogenesis by inhibiting VEGFR2 [5]. Likewise, mTOR signaling also acts as a pivotal mediator of angiogenesis, especially under hypoxia condition [8]. We examined the potential synergistic effect of rapamycin and cabozantinib on HUVECs. As expected, we found that combination treatment exhibited enhanced inhibition of vascular cell migration and tubule formation *in vitro* and angiogenesis *in vivo* than single drug. Moreover, activated mTOR signaling was found in anti-angiogenesis therapy-resistant cells [30], which provides more evidence for the synergistic effects of combination therapy.

Hypoxia induced by anti-angiogenic therapies initially retards cancer cell proliferation. Nevertheless, it also triggers the upregulation of a series of downstream genes of HIF1α, such as *VEGF* and *MET* [31,32]. Our previous data indicated that hypoxia induced the upregulation of cMet expression in cMet-low HCC cells, which increased the sensitivity to HGF stimulation and enhanced invasion ability. In this regard, cMet inhibitors could disrupt the aggressive phenotype induced by hypoxia [12]. This study

further revealed that, under hypoxia condition, rapamycin could further enhance the inhibitory effect of cabozantinib on HCC invasion even at a low level of cabozantinib.

Most of the previous preclinical trials examining therapeutic effects of cabozantinib on HCC were based on immunodeficient mouse models [5,33]. Considering that cMet and mTOR signaling are implicated in the establishment of a tumor microenvironment [11,34], we used immunocompetent mice and Hepa1-6 cells, proved to be resistant to cabozantinib *in vitro*, to explore the synergistic inhibitory effects of combination treatment *in vivo*. In Hepa1-6 xenografts, combination treatment showed significantly enhanced inhibition of tumor growth and angiogenesis than single inhibitor. In addition to the inhibitory effects on HCC cells, the mechanism underlying immune microenvironment regulation of the combination therapy needs further investigation.

Furthermore, besides cMet and VEGFR2, cabozantinib also targets other RTKs including RET, KIT, AXL, and FLT3 [5]. For instance, the growth arrest-specific protein 6/AXL signaling pathway and RET mutations have been implicated in the promotion of tumor cell proliferation, survival, migration, invasion, angiogenesis, and immune evasion [35,36]. Therefore, the synergistic effect of combination therapy on HCC cells may also be attributed to the modulation of these RTKs, which needs to be elucidated by further investigation.

In summary, our study identifies the mTOR inhibitor rapamycin as a feasible option to increase the sensitivity of cMet inhibitor-resistant HCC cells to cabozantinib. Rapamycin and cabozantinib exhibit synergistic inhibition of the proliferation and hypoxia-induced invasion of cMet inhibitor-resistant HCC cells and angiogenesis. Rapamycin along with other mTOR inhibitors is being evaluated in advanced-stage HCC clinical trials, and some have been approved in the treatment of different types of solid tumors [37]. Our data provide mechanistic evidence for the combination treatment of rapamycin and cabozantinib in treating HCC patients, especially for cMet inhibitor-resistant HCC patients.

Acknowledgements

This work was supported by grants from the National Key Project for Infectious Disease of China (No. 2017ZX10203207) and the National Natural Science Foundation of China (Nos. 81972737, 81930074, 91959203, and 81872356).

Compliance with ethics guidelines

Chao Gao, Shenghao Wang, Weiqing Shao, Yu Zhang, Lu Lu, Huliang Jia, Kejin Zhu, Jinhong Chen, Qiongzhu Dong, Ming Lu, Wenwei Zhu, and Lunxiu Qin declare that they have no conflict of interest. All procedures followed were in accordance with the ethical standards of the responsible committee on human experimentation (institutional and national) and with the *Helsinki Declaration* of 1975, as revised in 2000 (5). Informed consent was obtained from all patients for being included in the study. All institutional and national guidelines for the care and use of laboratory animals were followed.

Electronic Supplementary Material Supplementary material is available in the online version of this article at https://doi.org/10.1007/s11684-021-0869-y and is accessible for authorized users.

References

1. Bray F, Ferlay J, Soerjomataram I, Siegel RL, Torre LA, Jemal A. Global cancer statistics 2018: GLOBOCAN estimates of incidence and mortality worldwide for 36 cancers in 185 countries. CA Cancer J Clin 2018; 68(6): 394–424
2. Villanueva A. Hepatocellular carcinoma. N Engl J Med 2019; 380 (15): 1450–1462
3. Yang JD, Hainaut P, Gores GJ, Amadou A, Plymoth A, Roberts LR. A global view of hepatocellular carcinoma: trends, risk, prevention and management. Nat Rev Gastroenterol Hepatol 2019; 16(10): 589–604
4. Maroun CR, Rowlands T. The Met receptor tyrosine kinase: a key player in oncogenesis and drug resistance. Pharmacol Ther 2014; 142(3): 316–338
5. Yakes FM, Chen J, Tan J, Yamaguchi K, Shi Y, Yu P, Qian F, Chu F, Bentzien F, Cancilla B, Orf J, You A, Laird AD, Engst S, Lee L, Lesch J, Chou YC, Joly AH. Cabozantinib (XL184), a novel MET and VEGFR2 inhibitor, simultaneously suppresses metastasis, angiogenesis, and tumor growth. Mol Cancer Ther 2011; 10(12): 2298–2308
6. Abou-Alfa GK, Meyer T, Cheng AL, El-Khoueiry AB, Rimassa L, Ryoo BY, Cicin I, Merle P, Chen Y, Park JW, Blanc JF, Bolondi L, Klümpen HJ, Chan SL, Zagonel V, Pressiani T, Ryu MH, Venook AP, Hessel C, Borgman-Hagey AE, Schwab G, Kelley RK. Cabozantinib in patients with advanced and progressing hepatocellular carcinoma. N Engl J Med 2018; 379(1): 54–63
7. Llovet JM, Montal R, Sia D, Finn RS. Molecular therapies and precision medicine for hepatocellular carcinoma. Nat Rev Clin Oncol 2018; 15(10): 599–616
8. Faivre S, Kroemer G, Raymond E. Current development of mTOR inhibitors as anticancer agents. Nat Rev Drug Discov 2006; 5(8): 671–688
9. Chiarini F, Evangelisti C, McCubrey JA, Martelli AM. Current treatment strategies for inhibiting mTOR in cancer. Trends Pharmacol Sci 2015; 36(2): 124–135
10. Carracedo A, Ma L, Teruya-Feldstein J, Rojo F, Salmena L, Alimonti A, Egia A, Sasaki AT, Thomas G, Kozma SC, Papa A, Nardella C, Cantley LC, Baselga J, Pandolfi PP. Inhibition of mTORC1 leads to MAPK pathway activation through a PI3K-dependent feedback loop in human cancer. J Clin Invest 2008; 118 (9): 3065–3074
11. Saxton RA, Sabatini DM. mTOR signaling in growth, metabolism, and disease. Cell 2017; 168(6): 960–976
12. Zhang Y, Gao X, Zhu Y, Kadel D, Sun H, Chen J, Luo Q, Sun H, Yang L, Yang J, Sheng Y, Zheng Y, Zhu K, Dong Q, Qin L. The dual blockade of MET and VEGFR2 signaling demonstrates

pronounced inhibition on tumor growth and metastasis of hepatocellular carcinoma. J Exp Clin Cancer Res 2018; 37(1): 93
13. Chou TC. Drug combination studies and their synergy quantification using the Chou-Talalay method. Cancer Res 2010; 70(2): 440–446
14. Gherardi E, Birchmeier W, Birchmeier C, Vande Woude G. Targeting MET in cancer: rationale and progress. Nat Rev Cancer 2012; 12(2): 89–103
15. D'Errico A, Fiorentino M, Ponzetto A, Daikuhara Y, Tsubouchi H, Brechot C, Scoazec JY, Grigioni WF. Liver hepatocyte growth factor does not always correlate with hepatocellular proliferation in human liver lesions: its specific receptor c-met does. Hepatology 1996; 24(1): 60–64
16. Kaposi-Novak P, Lee JS, Gòmez-Quiroz L, Coulouarn C, Factor VM, Thorgeirsson SS. Met-regulated expression signature defines a subset of human hepatocellular carcinomas with poor prognosis and aggressive phenotype. J Clin Invest 2006; 116(6): 1582–1595
17. Rimassa L, Assenat E, Peck-Radosavljevic M, Zagonel V, Pracht M, Caremoli ER, Mathurin P, Harris WP, Bolondi L, Reig M, Damjanov N, Daniele B, Porta C, Mazzaferro V, Abbadessa G, Schwartz BE, Lamar M, Goldberg TR, Santoro A, Bruix J. Second-line tivantinib (ARQ 197) vs placebo in patients (Pts) with MET-high hepatocellular carcinoma (HCC): Results of the METIV-HCC phase III trial. J Clin Oncol 2017; 35(15 suppl): 4000
18. Hanahan D, Weinberg RA. Hallmarks of cancer: the next generation. Cell 2011; 144(5): 646–674
19. Dagogo-Jack I, Shaw AT. Tumour heterogeneity and resistance to cancer therapies. Nat Rev Clin Oncol 2018; 15(2): 81–94
20. Li X, Lewis MT, Huang J, Gutierrez C, Osborne CK, Wu MF, Hilsenbeck SG, Pavlick A, Zhang X, Chamness GC, Wong H, Rosen J, Chang JC. Intrinsic resistance of tumorigenic breast cancer cells to chemotherapy. J Natl Cancer Inst 2008; 100(9): 672–679
21. Bruix J, da Fonseca LG, Reig M. Insights into the success and failure of systemic therapy for hepatocellular carcinoma. Nat Rev Gastroenterol Hepatol 2019; 16(10): 617–630
22. Ezzoukhry Z, Louandre C, Trécherel E, Godin C, Chauffert B, Dupont S, Diouf M, Barbare JC, Mazière JC, Galmiche A. EGFR activation is a potential determinant of primary resistance of hepatocellular carcinoma cells to sorafenib. Int J Cancer 2012; 131(12): 2961–2969
23. Chiang DY, Villanueva A, Hoshida Y, Peix J, Newell P, Minguez B, LeBlanc AC, Donovan DJ, Thung SN, Solé M, Tovar V, Alsinet C, Ramos AH, Barretina J, Roayaie S, Schwartz M, Waxman S, Bruix J, Mazzaferro V, Ligon AH, Najfeld V, Friedman SL, Sellers WR, Meyerson M, Llovet JM. Focal gains of VEGFA and molecular classification of hepatocellular carcinoma. Cancer Res 2008; 68(16): 6779–6788
24. Hoshida Y, Nijman SM, Kobayashi M, Chan JA, Brunet JP, Chiang DY, Villanueva A, Newell P, Ikeda K, Hashimoto M, Watanabe G, Gabriel S, Friedman SL, Kumada H, Llovet JM, Golub TR. Integrative transcriptome analysis reveals common molecular subclasses of human hepatocellular carcinoma. Cancer Res 2009; 69(18): 7385–7392
25. Boyault S, Rickman DS, de Reyniès A, Balabaud C, Rebouissou S, Jeannot E, Hérault A, Saric J, Belghiti J, Franco D, Bioulac-Sage P, Laurent-Puig P, Zucman-Rossi J. Transcriptome classification of HCC is related to gene alterations and to new therapeutic targets. Hepatology 2007; 45(1): 42–52
26. Laplante M, Sabatini DM. mTOR signaling in growth control and disease. Cell 2012; 149(2): 274–293
27. Asnaghi L, Bruno P, Priulla M, Nicolin A. mTOR: a protein kinase switching between life and death. Pharmacol Res 2004; 50(6): 545–549
28. Villanueva A, Chiang DY, Newell P, Peix J, Thung S, Alsinet C, Tovar V, Roayaie S, Minguez B, Sole M, Battiston C, Van Laarhoven S, Fiel MI, Di Feo A, Hoshida Y, Yea S, Toffanin S, Ramos A, Martignetti JA, Mazzaferro V, Bruix J, Waxman S, Schwartz M, Meyerson M, Friedman SL, Llovet JM. Pivotal role of mTOR signaling in hepatocellular carcinoma. Gastroenterology 2008; 135(6): 1972–1983.e1–11
29. Imura Y, Yasui H, Outani H, Wakamatsu T, Hamada K, Nakai T, Yamada S, Myoui A, Araki N, Ueda T, Itoh K, Yoshikawa H, Naka N. Combined targeting of mTOR and c-MET signaling pathways for effective management of epithelioid sarcoma. Mol Cancer 2014; 13(1): 185
30. Wigerup C, Påhlman S, Bexell D. Therapeutic targeting of hypoxia and hypoxia-inducible factors in cancer. Pharmacol Ther 2016; 164: 152–169
31. Pugh CW, Ratcliffe PJ. Regulation of angiogenesis by hypoxia: role of the HIF system. Nat Med 2003; 9(6): 677–684
32. Semenza GL. Hypoxia-inducible factors: mediators of cancer progression and targets for cancer therapy. Trends Pharmacol Sci 2012; 33(4): 207–214
33. You H, Ding W, Dang H, Jiang Y, Rountree CB. c-Met represents a potential therapeutic target for personalized treatment in hepatocellular carcinoma. Hepatology 2011; 54(3): 879–889
34. Finisguerra V, Di Conza G, Di Matteo M, Serneels J, Costa S, Thompson AA, Wauters E, Walmsley S, Prenen H, Granot Z, Casazza A, Mazzone M. MET is required for the recruitment of anti-tumoural neutrophils. Nature 2015; 522(7556): 349–353
35. Zhu C, Wei Y, Wei X. AXL receptor tyrosine kinase as a promising anti-cancer approach: functions, molecular mechanisms and clinical applications. Mol Cancer 2019; 18(1): 153
36. Li AY, McCusker MG, Russo A, Scilla KA, Gittens A, Arensmeyer K, Mehra R, Adamo V, Rolfo C. RET fusions in solid tumors. Cancer Treat Rev 2019; 81: 101911
37. Janku F, Yap TA, Meric-Bernstam F. Targeting the PI3K pathway in cancer: are we making headway? Nat Rev Clin Oncol 2018; 15(5): 273–291